Hindawi
Journal of Sensors
Volume 2018, Article ID 6525919, 9 pages
https://doi.org/10.1155/2018/6525919

Research Article

NADH Oxidation onto Different Carbon-Based Sensors: Effect of Structure and Surface-Oxygenated Groups

Lucas Blandón-Naranjo,[1] Jorge Hoyos-Arbeláez,[1] Mario V. Vázquez,[1] Flavio Della Pelle,[2] and Dario Compagnone[2]

[1]*Grupo Interdisciplinario de Estudios Moleculares (GIEM), Instituto de Química, Universidad de Antioquia, Calle 67 No. 53–108 A.A 1226, Medellín, Colombia*
[2]*Faculty of Bioscience and Technology for Food, Agriculture and Environment, University of Teramo, 64023 Teramo, Italy*

Correspondence should be addressed to Mario V. Vázquez; mario.vazquez@udea.edu.co
and Dario Compagnone; dcompagnone@unite.it

Received 7 September 2017; Accepted 13 December 2017; Published 22 March 2018

Academic Editor: Maria Luz Rodríguez-Méndez

Different carbon-based materials have been compared for the development of NADH sensors: glassy carbon electrodes (GCE), multiwalled carbon nanotubes (MWCNT), and carbon black (CB). The GCE and MWCNT has been subjected to oxidative pretreatment to study the influence of oxidative groups for NADH oxidation. The materials had been characterized by FT-IR to identify the surface composition. The response of bare (GC) and GC/modified electrodes toward potassium ferricyanide have been employed to obtain information about the electroactive area and electron transfer rate. Studies of NAD^+/NADH redox behavior showed that MWCNT and GCE exhibit high degree of passivation while CB shows no fouling effects. Catalytic effect of surface-oxygenated groups was also proved for GCE and MWCNT, and both, O-GCE and O-MWCNT, exhibited a lower oxidation overpotential compared to the respective untreated materials. Chronoamperometric quantification showed a linear dependence between 2–18 $\mu mol \cdot L^{-1}$ and a detection limits of 6.2 $\mu mol \cdot L^{-1}$ (GCE), 5.4 $\mu mol \cdot L^{-1}$ (O-GCE), 3.2 $\mu mol \cdot L^{-1}$ (GCE/CB), 9.6 $\mu mol \cdot L^{-1}$ (GCE/MWCNT), and 4.9 $\mu mol \cdot L^{-1}$ (GCE/O-MWCNT) were obtained. The analytical performances suggest that a careful choice of the material for NADH sensing is necessary depending on the sensor application.

1. Introduction

The electrochemical behavior of NADH/NAD^+ redox couple has been widely studied because of the importance of this compound as cofactor in several biochemical processes. Oxidation of NADH occurs at high anodic overpotentials employing the most common electrode materials (i.e., glassy carbon and graphite) and implies the transfer of 2 electrons and one proton and the formation of NAD^+ molecule, which is reduced at high cathodic overpotentials for regenerating NADH molecule [1–3].

A significant decrease in the overpotential for NADH oxidation has been achieved using carbon-based nanomaterials. Different studies have demonstrated that oxygen-rich groups and quinone-like structures formed on the surface of carbon-based materials can promote the oxidation rate of NADH, working as "redox mediators" in electron transfer [1, 4–6]. Materials such as glassy carbon (GC), multiwalled carbon nanotubes (MWCNT), graphite, pyrolytic graphite (PG), graphene, and carbon black (CB) have been proposed as electrodes for NADH sensing [2, 5, 7–10]. All these materials are based on carbon; however, properties such as crystallinity, electron conductivity, hardness, and surface functional groups are significantly different. GC is a nongraphitizable carbon, combining glassy and ceramic properties of graphite. The structure obtained is generally as randomly intertwined ribbons of graphitic planes not presenting many functional groups at its surface beyond alkyl and aromatic groups, which are characteristic of the graphitic planes [11]. On the other hand, electrochemical oxidation of GC in basic or

acidic media has been tested as a surface modification methodology and has been demonstrated that heterogeneous transfer constant and capacitance are increased [12]. Multiwalled carbon nanotubes (MWCNTs) are cylindrical graphite-based molecules which have unusual properties, exploitable in areas like nanotechnology, electronics, optics, and other fields of material science and technology. MWCNTs have sp2-carbon units with few nanometers in diameter and many microns in length which allow surface modification with several functional groups [5, 13–15]. Carbon black (CB) is a nanomaterial produced by the incomplete combustion of heavy petroleum products such as coal tar, ethylene cracking tar, and a small amount from vegetable oil. The chemical and physical properties of carbon black are strongly influenced by the presence of surface oxides formed during the manufacturing process. Typically, CB has a graphitic-based structure characterized by a large number of defect sites which facilitate the presence of different functional groups as carboxylates, quinones, phenols, and aldehydes [9, 11, 16]. CB consists of spherical carbon primary particles, which typically form aggregates of ten or more spheres. The production of a stable CB nanodispersion is affordable and does not require sophisticated instrumentation [17]. Thus, CB has been largely used as a nanomaterial in sensing and biosensing [18, 19]. Nevertheless, studies about NADH electrochemical response over these materials are mainly focused on the catalytic activity, disregarding adsorption effects of oxidation products and fouling of electrode surface.

Depending on the electrode material, it has been demonstrated that NAD^+ produced from NADH oxidation can be strongly adsorbed on the electrode surface, causing fouling and loss of electrochemical response. This behavior limits the use of sensors for practical applications and suggest using them as disposable. The adsorption of NADH onto surface electrodes has been well studied by Elving at the end of the 1970s and the beginning of the 1980s [1, 4]. In these studies, Elving reported the adsorption phenomena of NAD^+ and the possibility of the formation of a $(NAD)_2$ dimer in the reduction step according to the reaction $2NAD^+ + 2e^- \rightarrow (NAD)_2$. The oxidation of the dimer is responsible for the appearance of an oxidation peak at lower anodic potentials with respect to the main oxidation process [1, 4].

The majority of studies of NADH oxidation are focused on the oxidation processes, while NAD^+ adsorption and reduction are not widely studied and the decrease in electrochemical response over reused electrodes is not commonly reported.

In this work, a careful comparison study of the electrochemical behavior of NAD^+/NADH redox couple has been carried out for sensors made of different materials: the classical glassy carbon and the recently widely used nanomaterial CB and MWCNTs. The aim was to properly correlate the electrochemical activity of NADH with the presence of oxygenated groups over the surface of the sensors and to understand the electrode surface modification during the sensing process. The study demonstrated that for complex redox reaction different considerations are needed to select the best material for the development of the appropriate sensors.

2. Materials and Methods

2.1. Chemicals and Solutions. Carbon-based materials used in this research were glassy carbon electrodes (GCE, CH Instruments Inc.), multiwalled carbon nanotubes (MWCNT), and carboxylate-modified MWCNT (O-MWCNT), supplied by Nano-Lab (EE.UU); carbon black (CB type N220 from Cabot Corporation, Ravenna, Italy).

β-Nicotinamide adenine dinucleotide reduced disodium salt hydrate (NADH, Santa Cruz Biotechnology.) NaH_2PO_4, Na_2HPO_4, KCl, ethanol, and potassium ferricyanide (K3[Fe(CN)6]) were of analytical grade and were from Sigma Aldrich Ultrapure water ($\rho = 18.2\,M\Omega{\cdot}cm$) from a Millipore-Milli-Q system was used for preparing all aqueous solutions.

2.2. Electrochemical Measurements. All electrochemical measurements were carried out with a Metrohm-Autolab PGSTAT101 potentiostat-galvanostat. Typical three electrode configuration composed of GCE and modified GCE, Ag/AgCl, and Pt wire as working, reference, and counter electrodes, respectively, was used.

2.3. Preparation of Electrodes. The GCE was polished with alumina powder of different size (1, 0.3, and 0.05 μm), 3 min each step, rinsed with Milli-Q water, dried with nitrogen, and cycled 10 times in PBS in the same potential range of the measurement to be carried out. O-GCE was obtained by electrochemical oxidation in basic media (KOH 1 M) according to the procedure reported by Anjo et al. [20]. Oxidation was carried out by fixing the potential at 1.2 V for 5 minutes until a stable current signal was achieved.

CB and O-MWCNT were suspended in Milli-Q water and sonicated for 2 hours until a stable $1\,mg{\cdot}mL^{-1}$ dispersion was obtained. The same protocol was carried out for MWCNT using ethanol as solvent. The preparation of GCE/CB, GCE/MWCNT, and GCE/O-MWCNT was carried out by one drop casting of 10 μL of each dispersion onto polished and cycled GCE electrodes and drying at room temperature.

2.4. Physicochemical Characterization of Carbon-Based Materials. Samples were characterized using qualitative infrared spectroscopy analysis in a Nicolet 6700 spectrometer, equipped with an MCT/A detector, and operated in a wavenumber ranging from $800\,cm^{-1}$ to $4000\,cm^{-1}$. For MWCNT, O-MWCNT, and CB, pellets were prepared with a sample/KBr weight ratio of 1/3000. Samples and pellets were heated, before the analysis, at 150°C in order to remove the water. For GCE and O-GCE, an ATR module was used.

The effective working area of the electrodes was determined from the slopes obtained for the graphs of I_p versus $v^{1/2}$ and using the Randles-Sevcik relationship for the one-electron redox process of $1\,mmol{\cdot}L^{-1}$ K3[Fe(CN)6] at scan rates of 5, 10, 20, 40, 60, 80, 100, and $150\,mV{\cdot}s^{-1}$, using the following parameters: diffusion coefficient $(D) = 7.60 \times 10^{-6}\ cm^2{\cdot}s^{-2}$, number of electrons transferred $(n) = 1$, and concentration $(C) = 1.0 \times 10^{-6}\,mol{\cdot}cm^{-3}$ (equivalent to $1\,mmol{\cdot}L^{-1}$) [21, 22].

The heterogeneous rate constants (k^0) were calculated from the difference of anodic and cathodic peak potentials, obtained for the same experiments used to obtain the electroactive area. The Nicholson method [23] was used, considering α equal to 0.5 (owing to the fact that I_{pa}/I_{pc} value is very close to unity). (I_{pa}: anodic peak current; I_{pc}: cathodic peak current).

2.5. NADH Measurements. Cyclic voltammetry (CV) at different potential ranges and scan rates were performed. Chronoamperometric (CA) experiments were carried out by fixing oxidation potentials according to the cyclic voltammetric data.

Plots of scan rate and the square root of scan rate were compared versus peak current in order to verify the type of electrochemical control of the NADH oxidation over the carbon-based materials. After each scan rate, every electrode was carefully washed with Milli-Q water in order to remove NADH oxidation products. Finally, chronoamperometric curves were obtained for NADH concentrations in the range of 2–18 μmol·L^{-1} by adding aliquots of NADH in PBS solution under constant stirring.

3. Results

3.1. Surface and Electrochemical Characterization of Carbon-Based Materials. FT-IR spectra obtained for the different carbon-based materials studied are reported in Figure 1. GC (Figure 1(a)) did not exhibit relevant signals; this is in agreement with the literature [11, 12]. The low-intensity band in the 3100–3400 cm^{-1} area can be related to the formation of -OH groups, and the signals at 1500–1700 cm^{-1} can be attributed to stretching of the carbonyl groups (Figure 1(b)). However, the very low absorption indicates the poor content of carbonyl and hydroxyl groups on the GC surface. This is was also obtained by Yi and coworkers [12].

MWCNTs and O-MWCNTs (Figure 1(c and e)) present significant differences. A band at 3470 cm^{-1} is present for O-MWCNT and can be attributed to OH stretching of carboxyl and hydroxyl groups. Both materials show signals in the range of 2950–2830 cm^{-1} that can be assigned to the stretching of C-H bonds (νC-H_2, C-H_3) of the carbon-based material. Bands at 1579 and 1576 cm^{-1} refer to C=C from aromatics. Absorption in the 1400 cm^{-1}—1050 cm^{-1} range corresponds to stretching of C-O, C-N aromatics, and aliphatics. The absence of bands at 3470 cm^{-1} and 1750–1630 cm^{-1} indicates no surface oxidation for MWCNT [11, 23]. The signal at 1545 cm^{-1} corresponds to the π bond between carbons. The absence of this band in GC and O-GC clearly demonstrates the difference in structural configuration between GC and MWCNT, oxidized or not [11].

CB spectra (Figure 1(d)) exhibit relevant signals at 3500 and 1200 cm^{-1} corresponding to hydroxyl groups and C-O stretching. Absorption at 1380 and 1050 cm^{-1} was also obtained; this can be assigned to the carboxylate groups. However, no band in the 1500–1800 cm^{-1} range was observed and is, then, not possible to confirm the presence of carbonyl groups. In this respect, it can be concluded that

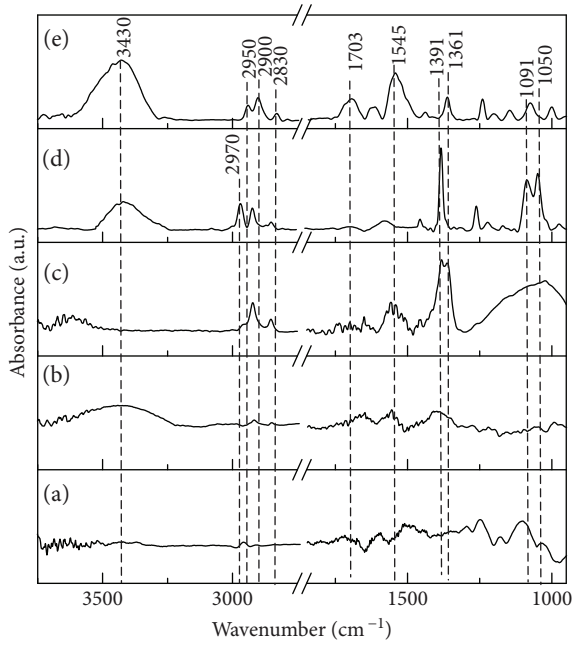

Figure 1: Infrared spectra for GC (a), O-GC (b), MWCNT (c), CB (d), and O-MWCNT (e).

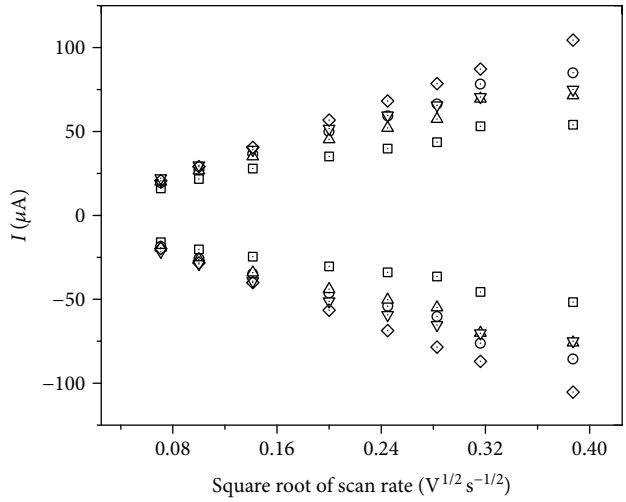

Figure 2: Anodic and cathodic peak currents versus square root of scan rate potential in potassium ferricyanide 1 mmol·L^{-1}, scan rates: 5, 10, 20, 40, 60, 80, 100, and 150 mV·s^{-1}. GCE (□), B O-GCE (○), GCE/CB (Δ), GCE/MWCNT (∇), and GCE/O-MWCNT (◊).

the main surface groups in CB are hydroxylic. Also, signals in the 2950–2830 cm^{-1} range typical of C-H bonds are present and can be attributed to CH_2 and CH_3 groups at the material surface [16].

Figure 2 reports the current peaks versus square root of scan rate plots, measured by cyclic voltammetry using ferro/ferricyanide redox couple for GCE, O-GCE, GCE/CB, GCE/MWCNT, and GCE/O-MWCNT. All electrodes exhibit good linearity for the anodic and cathodic current peaks as a function of the square root of the scan rate; this behavior indicates a semi-infinite linear diffusion-controlled current [21] for ferro/ferri cyanide reaction. According to

Table 1: Electroactive area and heterogeneous transfer constant obtained from ferro/ferricyanide redox couple.

	A (mm^2)	k^0 (cm·s^{-1} × 10^{-3})
GCE	16.03	1.9
O-GCE	29.23	4.5
GCE/CB	23.99	3.6
GCE/MWCNT	24.02	4.6
GCE/O-MWCNT	36.74	10.1

the Randles-Sevcik equation, the slope of every curve can be related with the electroactive area of the electrode [21, 22]. Also, Nicholson introduced a method to calculate k^0 (heterogeneous electron transfer constant) using the difference between oxidation and reduction potential at different scan rates. The values obtained are summarized in Table 1.

The smallest electrochemical area was obtained for GCE that is consistent with the lower value for k^0. O-GCE exhibited a larger area, owing to the treatment removing passive films over the material and giving active sites onto the electrode surface. This effect is more evident for k^0 value evidencing the increase of the electrochemical performances of the pretreated GC [20]. CB, MWCNT, and O-MWCNT are nanomaterials, and, for this reason, are expected that they have the larger areas. The large area obtained for GCE/O-MWCNT can be attributed to some imperfections caused by the oxidative treatment [24, 25]. k^0 values for CB and MWCNT are in the same order of magnitude, while the O-MWCNT rate is significantly high with respect to the other nanomaterials. Thus, oxygenated groups at the material surface apparently improve the process of charge transfer (O-GCE is higher than GCE, and O-MWCNT is higher than MWCNT). Taking into account that carbon nanotubes itself have high value of charge transfer, the presence of oxygenated groups onto nanotubes, as for O-MWCNT, explains the higher value for k^0.

3.2. Electrochemical Response for NADH Using Different Carbon-Based Materials. Figure 3 reports the cyclic voltammetries for NADH for all the studied materials. As expected, the anodic peak potential (Ep,a), corresponding to NADH oxidation, is different for all the materials tested. The highest Ep,a was obtained for GCE (0.698 V); a decrease of the potential needed for oxidation down to 0.464 V was observed for O-GCE. GCE/CB had Ep,a similar to O-GCE (0.442 V), while GCE/MWCNT (0.085) and GCE/O-MWCNT (0.054 V) had very low voltammetric anodic peaks. The decrease in oxidation overpotential and also the k^0 values reported in Table 1 implies a catalytic effect of the materials, being more significant for MWCNT and O-MWCNT, in agreement with the literature [2, 8, 25, 26]. The data obtained for GCE/CB are also in agreement with the literature, Arduini et al. [9] demonstrated, using a screen-printed electrode modified with CB, the CB ability to reduce the Ep,a for the NADH oxidation. In our case, the Ep,a reduction results more evident because of the intrinsic lower reactivity of GCE towards NADH. Surface oxidation improves the catalytic effect for NADH oxidation; this can be noticed looking

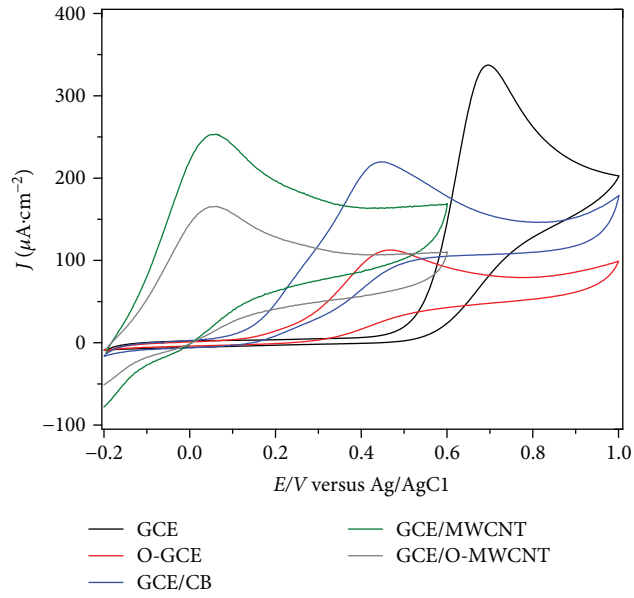

Figure 3: Cyclic voltammetry for different carbonaceous materials. Scan rate: 5 mV·s^{-1}, NADH concentration: 1 mmol·L^{-1}. C NADH: 1 mM; v: 5 mV·s^{-1}.

at the GCE/O-GCE and MWCNT/O-MWCNT pairs. The effect for NADH oxidation has been reported previously in the literature and is related to the interaction between the deprotonation step in NADH oxidation and the capacity of the oxygenated groups to accept the proton stabilizing the radical-cation formed [25, 27].

From cyclic voltammetry, it is possible to obtain an expression for heterogeneous transfer constant for the NADH oxidation process, using the correlation between the peak current (I_p) and the voltammetric charge (Q) at a fixed scan rate and analyte concentration.

In order to evaluate the type of electrochemical control for NADH oxidation on the electrodes surface, graphs of scan rate and the square root of scan rate versus I_p were built (Figure 4). Figure 4(a) reports the peak current as a function of the scan rate. It can be noted that only for GCE/MWCNTs and GCE/O-MWCNTs, a linear trend was obtained ($r^2 = 0.9960$ and 0.9939, resp.). Linearity is a characteristic of systems in which adsorption phenomena over electrode's surface have a major incidence in the electrochemical reaction. On the other hand, considering peak current versus square root of scan rate, linearity is found for GCE/O-GCE and GCE/CB ($r^2 = 0.9737$ and 0.9931, resp.). This is typical of reactions in which diffusion has more influence than the other kinds of kinetic controls on the electrochemical reaction. For GCE, linearity was not achieved by plotting peak current either versus scan rate or versus square root of scan rate; this indicates a mixed control type of reaction. Surface covering parameter (Γ) was calculated from the slope values obtained for MWCNT and O-MWCNT plots in Figure 4(a), based on the following.

$$I_p = \frac{n^2 F^2 \Gamma A v}{4RT}, \quad I_p \propto v, \tag{1}$$

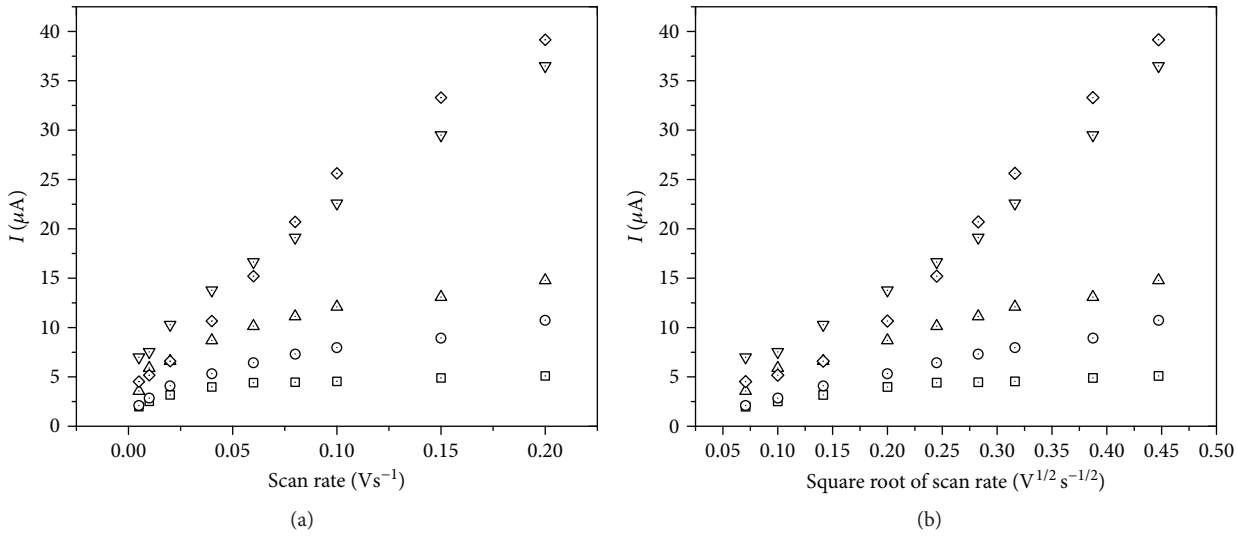

Figure 4: Anodic peak currents versus potential scan rate (a) and square root of potential scan rate (b). NADH concentration: 1 mmol·L^{-1}; scan rates: 5, 10, 20, 40, 60, 80, 100, 150, and 200 mV·s^{-1}. GCE (□), B O-GCE (○), GCE/CB (Δ), GCE/MWCNT (∇), and GCE/O-MWCNT (◊).

where I_p is the peak current, n is the number of transferred electrons, A is the electroactive area, C is the NADH concentration, v is the scan rate, Γ is the surface covering parameter, R is the gas constant, F is the Faraday constant, and T is the absolute temperature.

The surface covering parameters obtained for GCE/MWCNT and GCE/O-MWCNT were 4.17×10^{-7} and 3.43×10^{-7} μmol·mm^{-2}. This suggest that the MWCNT and O-MWCNT are probably equally affected by NAD^+ adsorbed after NADH oxidation.

Control of NADH oxidation for the different carbon-based materials tested resulted in different main control adsorption for the MWCNTs sensors, diffusion for O-GC and CB-GCE, and mixed control for O-GC. This is a key parameter in developing sensors since not only the chemical species reacting at the electrodes are significant but also the reaction product that can migrate to the bulk solution or remain adsorbed at the electrode surface. The latter case leads both to electrode passivation (fouling), which implies a decrease in the electroactive area, and in the decrease of electrocatalytic current for NADH oxidation. Evaluation of NAD^+ adsorption after NADH oxidation was carried out running 5 consecutive CVs (Figure 5) at 1 mmol·L^{-1}. GCE and GCE/CB (Figures 5(a) and 5(c)) did not exhibit any change for the anodic and cathodic peaks during the 5 cycle run confirming poor absorption of the reaction products. O-GCE (Figure 5(b)) exhibited a decrease of the oxidation peak current between first and second cycle, and after this cycle, the peak current remains stable; the cathodic potential peak has not significant variations. Figures 5(d) and 5(e), corresponding to GCE/MWCNT and GCE/O-MWCNT, show a different, and more complex, behavior compared with the other three sensors. During the first cycle, both materials exhibit one anodic and cathodic peak (2 and 2′). The anodic peak continuously decreases in function of the number of cycles while the cathodic continuously increases. Moreover, on the second cycle, a new anodic peak appears at 0.203 V for GCE/MWCNT and at −0.140 V for GCE/O-MWCNT (peak 1); the latter increases with CVs. Finally, an additional reduction peak at −0.830 V (1′) was found for MWCNT/GCE (Figure 5(d). In order to confirm that the peak 1 in Figures 5(d) and 5(e) depends on the reduction reaction (i.e., is the oxidation peak of the NAD dimer adsorbed and reduced at the electrode surface), cyclic voltammetries starting at lower cathodic potentials were run −0.7 V for GCE/MWCNT and −0.5 V for GCE/O-MWCNT (Figures 6(a) and 6(b)). The CVs confirmed that effectivity, peak 1 described in Figure 5, depends on the reduction reaction, since it disappeared in both cases.

According to these voltammograms, the following mechanism can be proposed for NADH/NAD^+ over GCE/MWCNT and GCE/O-MWCNT:

In the first anodic scan,

$$\mathrm{NADH} \rightarrow \mathrm{NAD^+} + \mathrm{H^+} + 2\mathrm{e^-}, \quad \text{peak 2} \tag{2}$$

Reduction process at the first cathodic scan

$$\begin{aligned} \mathrm{NAD^+} + \mathrm{e^-} &\rightarrow \mathrm{NAD^\bullet} \\ 2\mathrm{NAD^\bullet} &\rightarrow (\mathrm{NAD})_2 \end{aligned}, \quad \text{peak } 1' \qquad \mathrm{NAD^\bullet} + \mathrm{H^+} + \mathrm{e^-} \rightarrow \mathrm{NADH}, \quad \text{peak } 2' \tag{3}$$

Oxidation from the second scan onwards

$$\begin{aligned} (\mathrm{NAD})_2 &\rightarrow \mathrm{NAD^+} + 2\mathrm{e^-}, \quad \text{peak 1} \\ \mathrm{NADH} &\rightarrow \mathrm{NAD^+} + \mathrm{H^+} + 2\mathrm{e^-}, \quad \text{peak 2} \end{aligned} \tag{4}$$

The reported mechanism is very similar to that described by Moiroux and Elving [4] for NADH oxidation onto glassy carbon, pyrolytic graphite, and platinum.

Recent works for NADH oxidation studies onto chemically oxidized single-walled carbon nanotubes have shown experimental data in which two peaks are obtained for the oxidation process, but no discussion was reported [27]. All

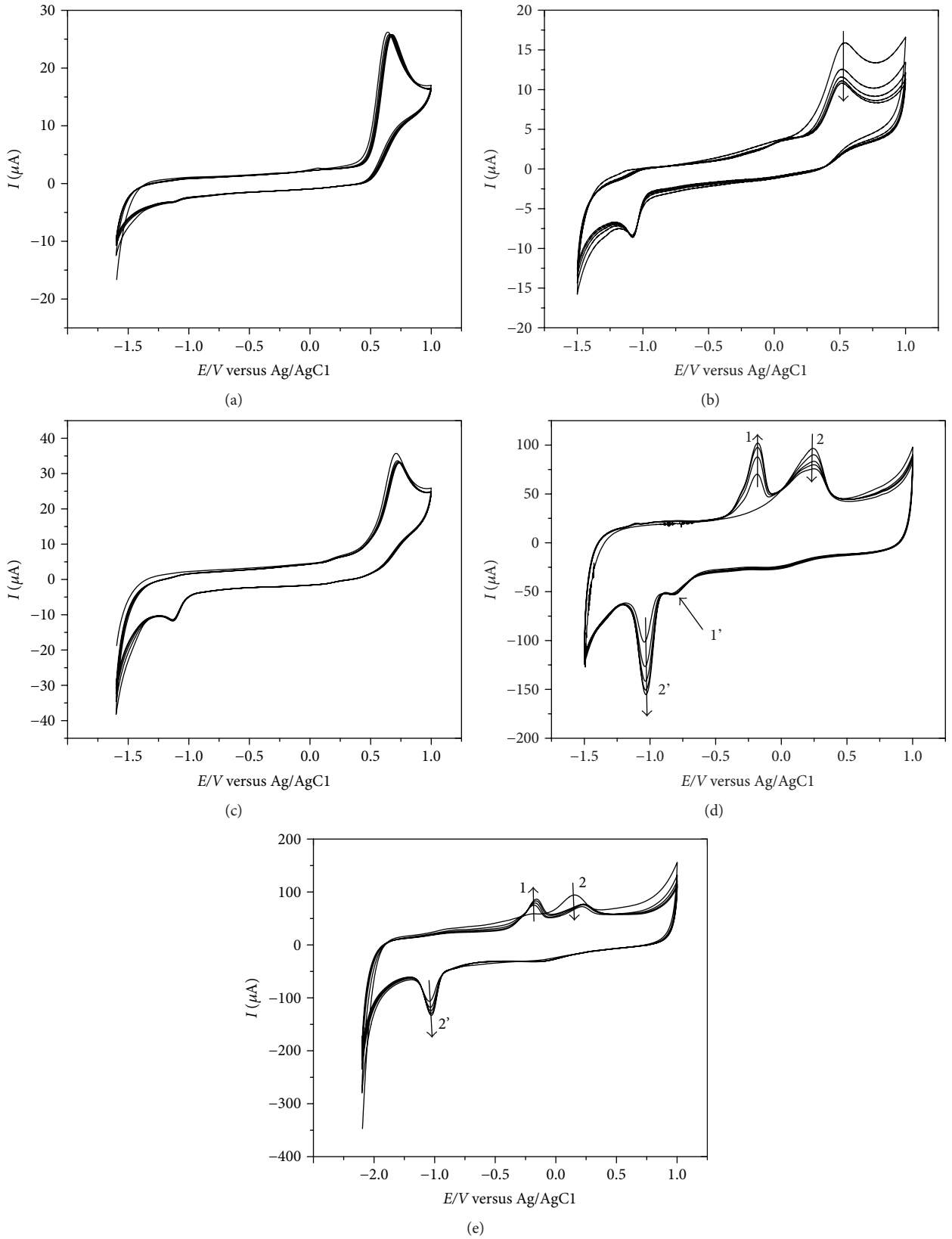

Figure 5: Cyclic voltammetries obtained for NADH over different carbonaceous materials. 5 cycles, $E_i = -1.6$ V, scan rate: 100 mV·s^{-1}. (a) GCE, (b) O-GCE, (c) GCE/CB, (d) GCE/MWCNT, and (e) GCE/O-MWCNT.

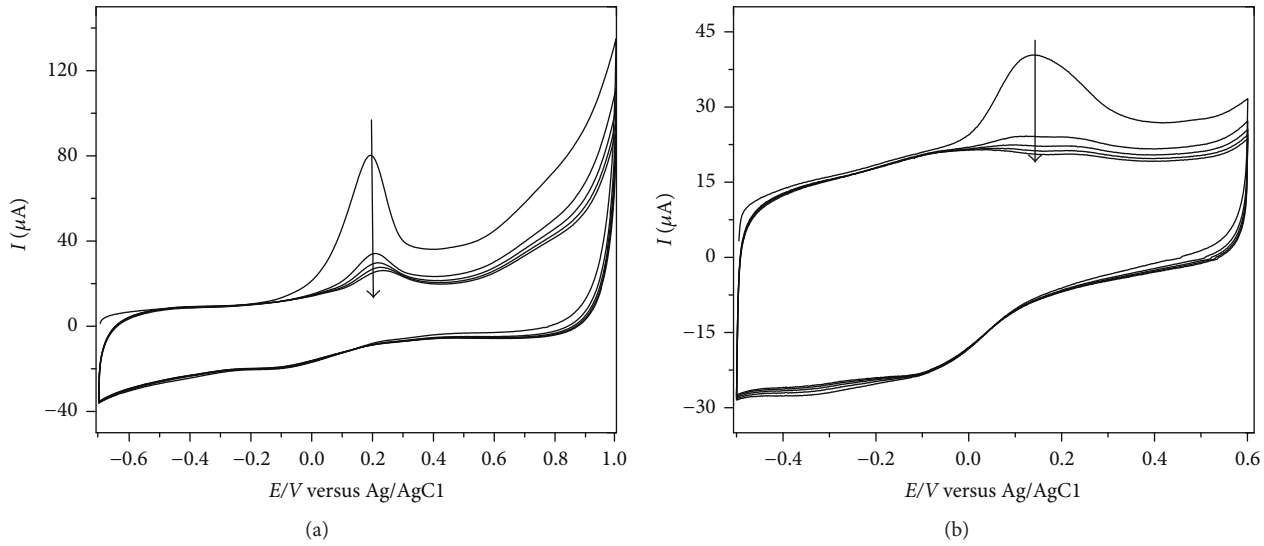

Figure 6: Cyclic voltammetries obtained for NADH over (a) GCE/MWCNT and (b) GCE/O-MWCNT at an initial potential before to the reduction potential peak. Scan rate: 100 $mV \cdot s^{-1}$, NADH concentration: 1 $mmol \cdot L^{-1}$.

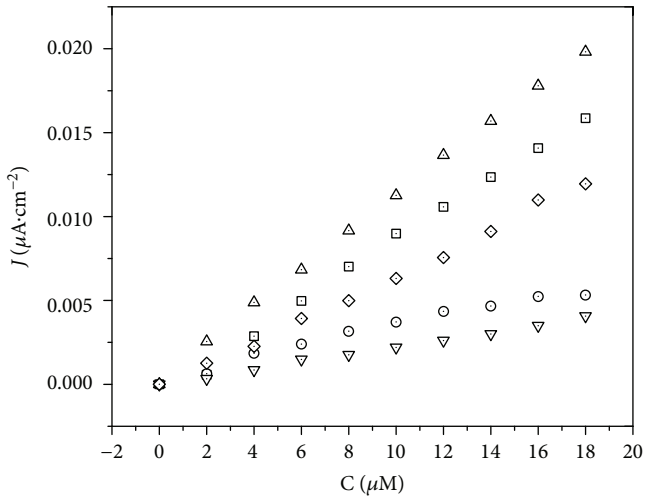

Figure 7: Calibration curve for NADH concentrations in the range of 2–18 $\mu mol \cdot L^{-1}$ obtained from chronoamperometric experiments over different carbonaceous materials and at different fixed potentials: GCE (□), O-GCE (○), GCE/CB (Δ), GCE/MWCNT (∇), and GCE/O-MWCNT (◊).

the data reported have shown that the NADH oxidation process using GCE/MWCNT and GCE/O-MWCNT is strongly subjected to adsorption and, then, rapid passivation of the electrode surface.

Finally, chronoamperometric experiments were carried out to check linearity of the current response in function of NADH concentration. Different fixed potentials were employed according to Ep,a obtained by voltagrams reported in Figure 3, and the same electrode was used under all the corresponding chronoamperometric experiment. Results are reported in Figure 7. Fouling is expected to have a strong effect on this kind of experiments, because the fixed potential implies the constant formation of NAD^+ on electrode surface for each NADH addition and also because each current point was obtained from the mean current data captured by 60 seconds which means that all the experiment was carried out by 10 minutes. According to this, the slope must be considerably affected as several NADH additions are made, causing a drop in the response current for the last additions.

Table 2: Parameters extracted from the calibration curve.

Material	Slope × 10^{-4} ($\mu A \cdot cm^2/\mu mol \cdot L^{-1}$)	R^2	LOD* ($\mu mol \cdot L^{-1}$)	LOQ** ($\mu mol \cdot L^{-1}$)
GCE	9.20	0.9957	6.2	31
O-GCE	3.05	0.9660	5.4	27
GCE/CB	11.1	0.9993	3.2	16
GCE/MWCNT	2.22	0.9960	9.6	47.5
GCE/O-MWCNT	6.73	0.9963	4.9	24.5

*LOD = blank signal + 3 *standard deviation of blank signal. **LOQ = blank signal + 5*standard deviation of blank signal.

Slope value, determination coefficient (r^2), limit of detection (LOD), and limit of quantification (LOQ) are presented in Table 2.

Satisfactory determination coefficients were observed for all sensors but there are significant differences in the slopes and limits of detection.

Highest slope and lowest detection limits were obtained for GCE/CB, indicating the good behavior of this material for NADH oxidation. On the other hand, the lowest slope was obtained for GCE/MWCNT with a high limit of detection compared with the other materials. This can be attributed to the passivation process after NADH oxidation which produces a decrease in the current response. Also, O-GCE exhibits a poor amperometric response and loss of linearity for the last points. This sensor did not exhibit the peaks due to dimer formation; however, the voltammogram (Figure 4(b)) exhibited a considerable decrease of the anodic

peak for the multiple scans indicating a decrease of the electroactive surface able to oxidize NADH. The good GCE/CB response is correlated, in our opinion, with nonfouling characteristics reported in this work despite the lower heterogeneous rate constant with respect to O-MWCNTs. Relative standard deviations obtained from 5 consecutive chronoamperometric measurements at a concentration of 10 μM NADH were as follows: 3.4% for GCE/CB, 4.1% for O-GCE, 2.4% for GC/CB, 3.8% for GC/MWCT, and 4.4% for GC/O-MWCT.

4. Conclusions

The electrochemical response of NADH of different sensors made of carbon-based materials has been evaluated. The effect of surface oxygen-rich functionalities and the type of structural proprieties of the material were related with catalytic effect for the NADH oxidation. According to the oxidation peaks obtained for NADH, oxygen-rich materials confers a catalytic effect for the oxidation of the molecule.

As expected, and reported in the literature, MWCNT and O-MWCNT exhibited the lowest potential for the oxidation and high catalytic activity. CB which has a graphite-based structure and nanometric size exhibited also good catalytic activity.

A study of the passivation of the sensors gave high passivation for GCE/MWCNT and GCE/O-MWCNT, probably due to the morphology of the material. Both materials showed the appearance of a cathodic peak that can be assigned to the formation of a $(NAD)_2$ dimer due to a strong NAD^+ adsorption over the surface of the electrode. Chronoamperometric measurement confirmed that passivation strongly influences the analytical behavior of the sensors indicating as the best sensor the CB-GCE despite the higher oxidation potential and lower heterogeneous rate constant with respect to O-MWCNTs. This study clearly demonstrates that a careful study is needed for the selection of the appropriate material to develop chemical sensors for organic compounds. This selection must not be only directed to assess the highest response or the lower applied potential useful for the redox reaction. Complex phenomena occurring at the electrode surface, as those reported in this paper for NADH oxidation, can result in the wrong choice of material and voltammetric technique used. For example, in the case reported, O-MWCNTs appear to be the best carbon-based material among those tested, but only if a very low applied potential is required for the analysis (i.e., analysis directed in a medium with potentially oxidizable interfering compounds) and it should be used as disposable sensor with a rapid voltammetric technique (i.e., differential pulse voltammetry). If the potential is low enough and it will be necessary to run calibration measurement cycles or to carry an analysis for few seconds or minutes (as for enzymatic analysis), the CB-GCE option would be definitively more applicable.

Conflicts of Interest

The authors declare that they have no conflicts of interest.

Acknowledgments

Lucas Blandón-Naranjo and Jorge Hoyos-Arbeláez would like to thank to COLCIENCIAS for the doctoral scholarship. Mario V. Vázquez would like to thank to CODI-University of Antioquia for the support of the Project 2015-7523. Flavio Della Pelle and Dario Compagnone acknowledge the financial contribution of the Italian Ministry of Foreign Affairs for the Project "materiali nanostrutturati per sistemi (bio) chimici sensibili ai pesticidi."

References

[1] P. J. Elving, W. T. Breshahan, J. Moiroux, and Z. Samec, "NAD/NADH as a model redox system: mechanism, mediation, modification by the environment," *Bioelectrochemistry and Bioenergetics*, vol. 9, no. 3, pp. 365–378, 1982.

[2] A. Radoi and D. Compagnone, "Recent advances in NADH electrochemical sensing design," *Bioelectrochemistry*, vol. 76, no. 1-2, pp. 126–134, 2009.

[3] A. J. Bard, M. Stratmann, Gileadi E., and M. Urbakh, *Encyclopedia of Electrochemistry, Thermodynamics and Electrified Interfaces*, vol. 1, pp. 1-2, Wiley-VCh, Weinheim, Germany, 2002.

[4] J. Moiroux and P. J. Elving, "Adsorption phenomena in the NAD^+/NADH system at glassy carbon electrodes," *Journal of Electroanalytical Chemistry and Interfacial Electrochemistry*, vol. 102, no. 1, pp. 93–108, 1979.

[5] A. Radoi, D. Compagnone, M. A. Valcarcel et al., "Detection of NADH via electrocatalytic oxidation at single-walled carbon nanotubes modified with variamine blue," *Electrochimica Acta*, vol. 53, no. 5, pp. 2161–2169, 2008.

[6] S. Cinti, F. Arduini, M. Carbone et al., "Screen-printed electrodes modified with carbon nanomaterials: a comparison among carbon black, carbon nanotubes and graphene," *Electroanalysis*, vol. 27, no. 9, pp. 2230–2238, 2015.

[7] M. A. Jensen and P. J. Elving, "244 - oxidation of 1,4-NADH at a glassy carbon electrode: effects of pH, lewis acids and adsorption," *Bioelectrochemistry and Bioenergetics*, vol. 5, no. 3, pp. 526–534, 1978.

[8] C. Zanardi, E. Ferrari, L. Pigani, F. Arduini, and R. Seeber, "Development of an electrochemical sensor for NADH determination based on a caffeic acid redox mediator supported on carbon black," *Chemosensors*, vol. 3, no. 2, pp. 118–128, 2015.

[9] F. Arduini, A. Amine, C. Majorani et al., "High performance electrochemical sensor based on modified screen-printed electrodes with cost-effective dispersion of nanostructured carbon black," *Electrochemistry Communications*, vol. 12, no. 3, pp. 346–350, 2010.

[10] L. Blandón-Naranjo, F. Della Pelle, M. V. Vázquez et al., "Electrochemical behaviour of microwave-assisted oxidized MWCNTs based disposable electrodes: proposal of a NADH electrochemical sensor," *Electroanalysis*, 2018.

[11] R. L. McCreery, "Advanced carbon electrode materials for molecular electrochemistry," *Chemical Reviews*, vol. 108, no. 7, pp. 2646–2687, 2008.

[12] Y. Yi, G. Weinberg, M. Prenzel et al., "Electrochemical corrosion of a glassy carbon electrode," *Catalysis Today*, vol. 295, pp. 32–40, 2017.

[13] M. Del Carlo, A. Amine, M. Haddam, F. Della Pelle, G. C. Fusella, and D. Compagnone, "Selective voltammetric analysis of *o*-diphenols from olive oil using Na_2MoO_4 as electrochemical mediator," *Electroanalysis*, vol. 24, no. 4, pp. 889–896, 2012.

[14] A. Gasnier, M. L. Pedano, F. Gutierrez, P. Labbé, G. A. Rivas, and M. D. Rubianes, "Glassy carbon electrodes modified with a dispersion of multi-wall carbon nanotubes in dopamine-functionalized polyethylenimine: characterization and analytical applications for nicotinamide adenine dinucleotide quantification," *Electrochimica Acta*, vol. 71, pp. 73–81, 2012.

[15] A. J. Saleh Ahammad, J.-J. Lee, and M. A. Rahman, "Electrochemical sensors based on carbon nanotubes," *Sensors*, vol. 9, no. 4, pp. 2289–2319, 2009.

[16] W. M. Prest and R. A. Mosher, "Fourier transform IR spectroscopic characterization of the functional groups on carbon black," in *Colloids and Surfaces in Reprographic Technology: ACS Symposium Series*, M. Hair and M. D. Croucher, Eds., American Chemical Society, Washington, DC, 1982.

[17] F. Della Pelle, L. Vázquez, M. Del Carlo, M. Sergi, D. Compagnone, and A. Escarpa, "Press-printed conductive carbon black nanoparticle films for molecular detection at the microscale," *Chemistry - A European Journal*, vol. 22, no. 36, pp. 12761–12766, 2016.

[18] F. Della Pelle, R. Di Battista, L. Vázquez et al., "Press-transferred carbon black nanoparticles for class-selective antioxidant electrochemical detection," *Applied Materials Today*, vol. 9, pp. 29–36, 2017.

[19] F. Della Pelle, M. Del Carlo, M. Sergi, D. Compagnone, and A. Escarpa, "Press-transferred carbon black nanoparticles on board of microfluidic chips for rapid and sensitive amperometric determination of phenyl carbamate pesticides in environmental samples," *Microchimica Acta*, vol. 183, no. 12, pp. 3143–3149, 2016.

[20] D. M. Anjo, M. Kahr, M. M. Khodabakhsh, S. Nowinski, and M. Wanger, "Electrochemical activation of carbon electrodes in base: minimization of dopamine adsorption and electrode capacitance," *Analytical Chemistry*, vol. 61, no. 23, pp. 2603–2608, 1989.

[21] A. J. Bard and L. R. Faulkner, *Electrochemical Methods: Fundamentals and Applications*, Wiley, New York, 2nd edition, 2001.

[22] J. Wang, *Analytical Electrochemistry*, John Wiley & Sons, Inc., New Jersey, Third edition, 2006.

[23] R. S. Nicholson, "Theory and application of cyclic voltammetry for measurement of electrode reaction kinetics," *Analytical Chemistry*, vol. 37, no. 11, pp. 1351–1355, 1965.

[24] V. Datsyuk, M. Kalyva, K. Papagelis et al., "Chemical oxidation of multiwalled carbon nanotubes," *Carbon*, vol. 46, no. 6, pp. 833–840, 2008.

[25] M. Wooten and W. Gorski, "Facilitation of NADH electrooxidation at treated carbon nanotubes," *Analytical Chemistry*, vol. 82, no. 4, pp. 1299–1304, 2010.

[26] E. Katekawa, F. Maximiano, L. L. Rodrigues, M. Flávia Delbem, and S. H. Serrano, "Electrochemical oxidation of NADH at a bare glassy carbon electrode in different supporting electrolytes," *Analytica Chimica Acta*, vol. 385, no. 1-3, pp. 345–352, 1999.

[27] M. Tominaga, A. Iwaoka, D. Kawai, and S. Sakamoto, "Correlation between carbon oxygenated species of SWCNTs and the electrochemical oxidation reaction of NADH," *Electrochemistry Communications*, vol. 31, pp. 76–79, 2013.